

A type of human skin dendritic cell marked by CD5 is associated with the development of inflammatory skin disease

Daniel Korenfeld,¹ Laurent Gorvel,¹ Adiel Munk,¹ Joshua Man,¹ Andras Schaffer,² Thomas Tung,³ Caroline Mann,⁴ and Eynav Klechevsky¹

¹Department of Pathology and Immunology, Division of Immunobiology, ²Department of Pathology and Immunology, Dermatopathology Center, ³Department of Surgery, Division of Plastic and Reconstructive Surgery, and ⁴Department of Medicine, Division of Dermatology, Washington University School of Medicine in St. Louis, St. Louis, Missouri, USA.

Dendritic cells (DCs) are important in regulating immunity and tolerance and consist of functionally distinct subsets that differentially regulate T lymphocyte function. The underlying basis for this subset specificity is lacking, particularly in humans, where the classification of tissue DCs is currently incomplete. Examination of healthy human epidermal Langerhans cells and dermal skin cells revealed a tissue CD5-expressing DC subtype. The CD5⁺ DCs were potent inducers of cytotoxic T cells and Th22 cells. The products of these T cells, IL-22 and IFN- γ , play a key role in the pathogenesis of psoriasis. Remarkably, CD5⁺ DCs were significantly enriched in lesional psoriatic skin compared with distal tissues, suggesting their involvement in the disease. We show that CD5⁺ DCs can be differentiated from hematopoietic progenitor cells independently of the CD5⁻ DCs. A progenitor population found in human cord blood and in the dermal skin layer, marked as CD34⁻CD123⁺CD117^{dim}CD45RA⁺, was an immediate precursor of these CD11c⁺CD1c⁺CD5⁺ DCs. Overall, our discovery of the CD5-expressing DC subtype suggests that strategies to regulate their composition or function in the skin will represent an innovative approach for the treatment of immune-mediated disorders in and beyond the skin.

Introduction

Dendritic cells (DCs) comprise a heterogeneous group of antigen-presenting cells (APCs) found throughout the body that include plasmacytoid DCs (pDCs) and CD11c myeloid DCs (mDCs) or conventional DCs (cDCs) (1). DC subsets display different cell surface markers that afford each specific DC population different functions (2). Consequently, normal immunity and tolerance are dependent on a balance among the DC subsets. In human skin, cDCs include epidermal Langerhans cells (LCs) and dermal CD1a^{dim}CD141⁻, dermal CD1a^{dim}CD141⁺, and dermal CD14⁺ subsets, which all have distinct functional properties (2–4). The dermal CD14⁺ DCs promote humoral immunity and regulate cellular immunity (5–10). In contrast, LCs enhance cellular immunity by inducing Th2 differentiation of naive CD4⁺ T cells and via priming and cross-priming of naive CD8⁺ T cells (5, 9, 11). Recently, human LCs were also shown to be responsible for directing IL-17- and IL-22-mediated responses (12–15), two responses indicative of inflammatory autoimmune skin diseases, such as psoriasis.

Emerging studies demonstrate critical roles for the DC subsets in the initiation and maintenance of psoriasis (16, 17). These are supported by the increased numbers of cytokine-producing DCs in psoriatic lesions and their role in inducing Th1 (IFN- γ , TNF- α , and Th17 [IL-17 and IL-22]) responses (18, 19). Novel antipsoriatic therapies, which specifically target inflammatory DC cytokines, bring better clinical improvement compared with conventional treatments and implicate the crucial importance of DCs in psoriasis pathogenesis (20, 21). Psoriatic inflammatory cDCs were described to include cells with reduced expression of CD1c (18) and a subset of DCs that produce TNF- α and iNOS (21). However, a detailed phenotype of the key DC that contributes to the priming of the inflammatory T cell response via Th1, Th17, or Th22 is still unknown (22).

Conflict of interest: The authors have declared that no conflict of interest exists.

Submitted: July 5, 2017

Accepted: August 10, 2017

Published: September 21, 2017

Reference information:

JCI Insight. 2017;2(18):e96101.

<https://doi.org/10.1172/jci.insight.96101>

insight.96101.

In this study, we extended the analysis of all the DC populations in human skin and discovered that LCs and dermal DCs are heterogeneous, containing terminally differentiating DCs that express CD5. CD5⁺ DCs are superior activators of inflammatory T cell responses. In addition, we revealed the presence of pre-CD5 DC precursor in human dermis. These data offer insights into human tissue DC heterogeneity and ontogeny and highlight unexplored avenues for investigation of the therapeutic potential of DC subset-specific targeting.

Results

CD5 marks a subset of epidermal LCs and dermal CD1a^{dim} DCs in healthy skin. Human skin is known to contain four distinct mDC subsets. Three of these, marked as CD1a^{dim}CD141⁻, CD1a^{dim}CD141⁺, or CD1a⁻CD14⁺, are found in the dermis, while CD1a^{hi}Langerin⁺ LCs are found in the epidermis (3, 23). To define unique surface markers and to fully characterize expression patterns of each epidermal and dermal subset, we performed a flow cytometry analysis of 332 different surface proteins. We found that both LCs and dermal CD1a^{dim}CD141⁻ DCs are heterogeneous in 33 tested donors containing distinct CD5⁺ and CD5⁻ populations (Figure 1, A and B). The CD5⁺ LCs fraction comprised a mean \pm SEM of 6% \pm 1.05% and the CD5⁺ DCs fraction in the dermis comprised 15.8% \pm 2.1% of skin DCs (Figure 1B). The CD5⁺ cells in both the epidermis and the dermis displayed DC morphology and were indistinguishable from their negative counterparts (Figure 1C). CD5 was not expressed on skin CD141-expressing cells, including dermal CD1a^{dim}CD141⁺ or dermal CD14⁺ DCs (Figure 1A; right). The CD5⁺ cells in both epidermis and dermis expressed CD1c (Supplemental Figure 1A; supplemental material available online with this article; <https://doi.org/10.1172/jci.insight.96101DS1>). Dermal CD5⁺ and CD5⁻ cells but not epidermal CD5⁺ and CD5⁻ cells expressed CD11b; conversely, only epidermal CD5⁺ and CD5⁻ cells, but not dermal CD5⁺ and CD5⁻ cells, expressed Langerin (Figure 1A, left, and Figure 1D). CD5 was also expressed on a subset of peripheral blood and cord blood CD11c⁺CD1c⁺ DCs but not on blood CD11c⁺CD141⁺ DCs (Supplemental Figure 1A). Skin CD5⁺ DCs expressed higher amounts of CD83, CD86, and CCR7 than blood CD5⁺ DCs. However, the expression of these markers was comparable to their skin CD5⁻ DCs counterparts. Because CD5 and CD6 are often coexpressed on the surface of T cells or B cells (24), the expression of CD6 on the surface of skin CD5⁺ DCs or skin-resident T cells was assessed. Interestingly, CD6 was absent from the surface of the DCs in the skin but was expressed on the surface of skin-resident T cells (Supplemental Figure 1B). This feature was shared with the blood CD1c⁺CD5⁺ DCs (Supplemental Figure 1C). Thus, CD5 marks a population of human skin LCs and dermal CD1a^{dim} DCs.

CD5 marks a stable terminally differentiated DC subset. One indication of whether CD5 demarcates a distinct cell fate of DCs, rather than just constituting an activation marker, would be its stability on the surface of a cell. Thus, the stability of CD5 expression on the DC was tested in culture. Indeed, after 6 days in culture, CD5 was present on the surface of CD5⁺ DCs and remained absent from the CD5⁻ DCs (Figure 1E, black histograms). To further assess whether CD5 marks a specific terminally differentiated cell fate, dermal CD5⁺ and CD5⁻ DCs were exposed for 6 days to a variety of stimuli, including Toll-like receptor (TLR-2, -3, -4) agonists, inflammatory or DC differentiating cytokines (IFN- γ , IFN- α , FLT3-L, granulocyte macrophage colony-stimulating factor [GM-CSF], IL-4), or a T cell signal (T cells, CD40L). Under these conditions, CD5 remained on the surface of the positive cells and its level of expression did not change significantly (Figure 1E, top, red histograms). Moreover, CD5 expression was not detected on the stimulated CD5⁻ DCs (Figure 1E, bottom, red histograms). Overall, these data demonstrate that CD5 marks a distinct and stable terminally differentiated DCs.

Dermal CD5⁺ DCs efficiently prime allogeneic naive CD8⁺ T cells. The biological properties of CD5⁺ DCs from the dermis were first assessed by measuring their capacity to prime cytotoxic T lymphocyte (CTL) responses. Sorted live HLA-DR⁺CD1a^{dim}CD5⁺ DCs or their CD5⁻ dermal counterparts were cocultured with allogeneic naive T cells and analyzed after 7 days for T cell proliferation. As shown in Figure 2, A and B, CD5⁺ DCs were more powerful stimulators of naive CD8⁺ T cell proliferation than the CD5⁻ DCs, as measured by the dilution of CFSE. Consistent with previous reports, dermal CD1a^{dim}CD141⁺ and CD14⁺ DCs served as controls and induced only weak CTL responses (Figure 2, A and B) (5, 25). CD8⁺ T cells primed with CD5⁺ dermal CD1a^{dim} DCs expressed higher levels of granzyme B compared with those primed with matched CD5⁻ DCs (Figure 2, B and C). Moreover, we observed greater expansion of IFN- γ - and TNF- α -producing CD8⁺ T cells by CD5⁺ dermal DCs, as measured intracellularly by flow cytometry (Figure 2D). Furthermore, CD8⁺ T cells that were primed by CD5⁺ dermal CD1a^{dim} DCs

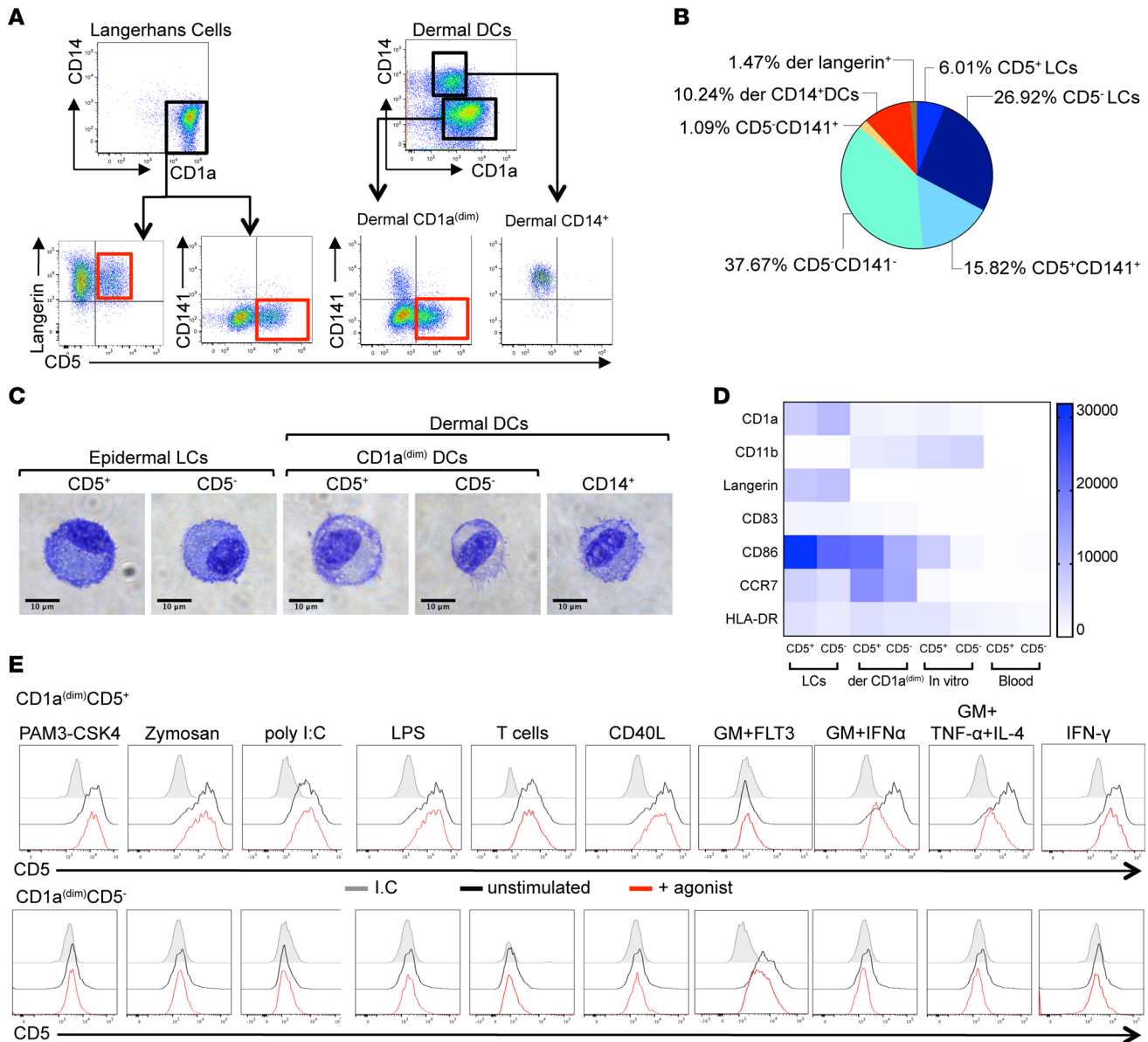


Figure 1. Identification of Langerhans cells and dermal DC subsets in human skin. (A) Top: Expression of CD1a and CD14 on purified skin DCs defines epidermal CD1a⁺ LCs, dermal CD1a^{dim} DCs, and dermal CD14⁺ DCs subpopulations. Bottom: Expression of CD5 defines subpopulations of CD1a^{hi}Langerin⁺ LCs and dermal CD1a^{dim}CD141⁻ DCs. **(B)** Relative representation of each human DC subset in normal skin (n = 33). The percentage of individual DC subsets mean \pm SD \pm SEM of the total migrating DCs (HLA-DR⁺CD3/19/56⁻) cells is plotted. Epidermal CD5⁺ LCs: 6.0% \pm 6.15% \pm 1.05%; CD5⁻ LCs: 26.9% \pm 20.4% \pm 3.4%; dermal CD1a^{dim} DCs, CD5⁺: 15.8% \pm 12.6% \pm 2.16%; CD5⁻: 37.6% \pm 18.9% \pm 3.2%; CD141⁺: 1.09% \pm 2% \pm 0.3%; dermal CD14⁺ DCs: 10.2% \pm 7.6% \pm 1.3%. **(C)** Morphology of sorted skin CD5⁺ LCs, CD5⁻ LCs, dermal CD1a^{dim}CD5⁺ DCs, CD1a^{dim}CD5⁻ DCs, CD1a^{dim}CD141⁺ DCs, and CD14⁺ DCs visualized by Giemsa staining. Scale bar: 10 μ M. **(D)** HLA-DR⁺CD11c⁺CD14⁻CD1c⁺CD5⁺ and CD5⁻ DCs from skin epidermis, dermis, blood, and in vitro-differentiated cultures were analyzed for the expression of CD1a, CD11b, Langerin, CD83, CD86, CCR7, and HLA-DR. The plot shows GeoMean intensity, with values of the background staining subtracted. The mean values obtained for 2–4 donors are plotted. **(E)** Dermal CD1a^{dim}CD5⁺ and CD5⁻ DCs were sorted and stimulated as indicated. Histograms show expression of CD5 on the cells after 6 days of stimulation (red histograms). One representative of 3 donors is shown.

produced more IFN- γ compared with the cells primed by the CD5⁻ dermal CD1a^{dim} DCs, as measured in culture supernatant per cell (Figure 2E). Overall, our data show that the CD5⁺ DC subset is specialized in driving multifunctional CD8⁺ T cell immunity.

Dermal CD5⁺ DCs polarize naive CD4⁺ T cells into Th1 and Th22 cells. To address whether CD5⁺ DC populations play a specific role in inducing the differentiation of T helper cell subsets, we cocultured sorted dermal CD5⁺ or CD5⁻ DCs with allogeneic naive T cells. After 6–8 days, dermal CD5⁺ DCs induced higher levels of CFSE dilution compared with their CD5⁻ counterparts (Figure 3A). Dermal CD14⁺ DCs and dermal CD1a^{dim}CD141⁺ DCs served as controls and were the weakest stimuli for proliferation (Figure 3A).

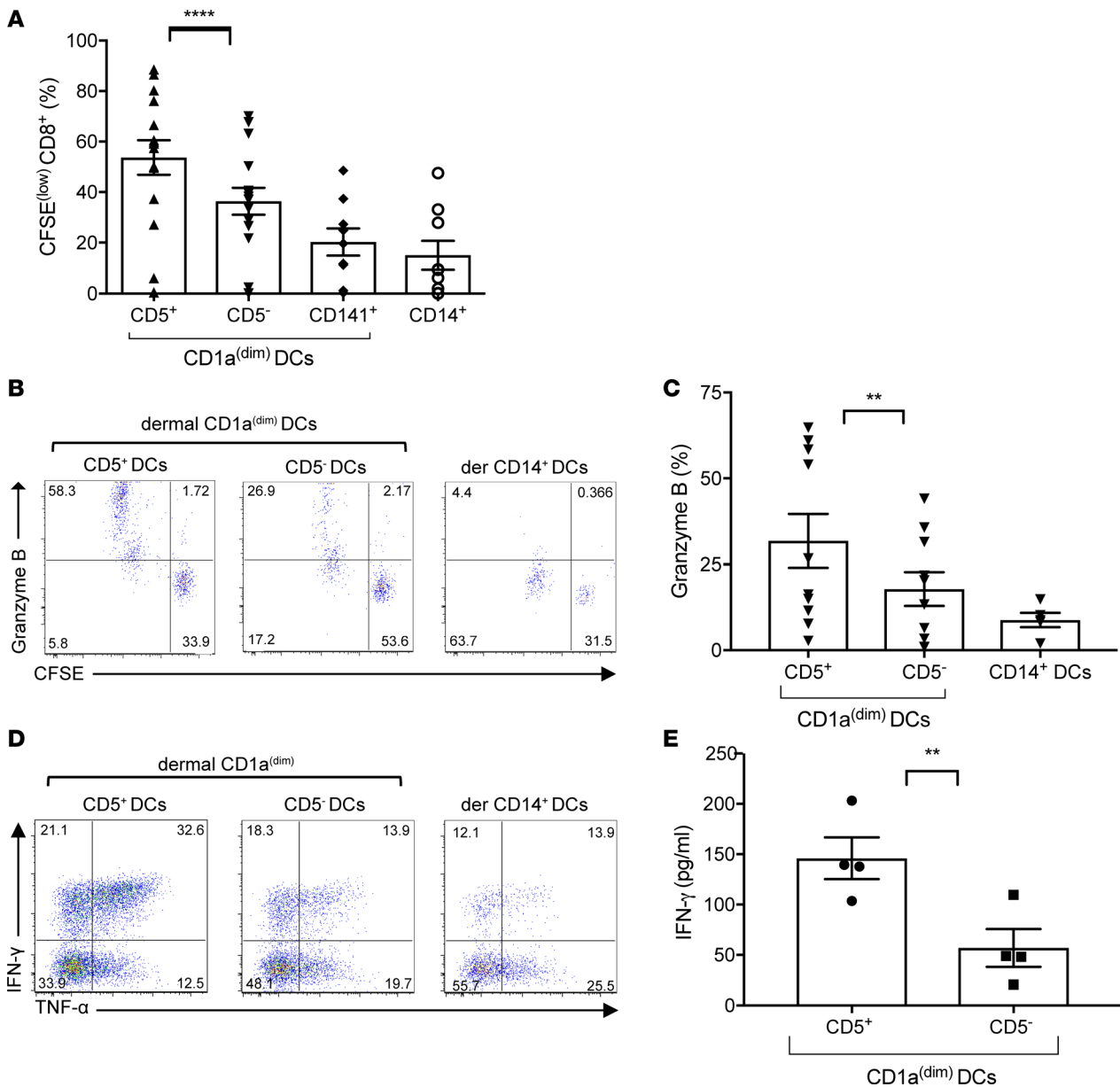


Figure 2. Dermal CD5⁺ DCs are more efficient than their CD5⁻ counterparts at priming CTLs. (A) Allogeneic naive CD8⁺ T cells primed with sorted CD40L-activated skin dermal CD5⁺ or CD5⁻ CD1a^{dim} DCs, dermal CD1a^{dim}CD141⁺ DCs, or dermal CD14⁺ DCs at ratio 1:40 for 7 days. The graph shows the percentage of proliferating (CFSE^{low}) CD3⁺CD8⁺ T cells (*n* = 15). Mean ± SD ± SEM for CD5⁺: 53.7% ± 26.6% ± 6.8%, CD5⁻: 36.4% ± 20.7% ± 5.3%, CD141⁺ DCs: 20.2% ± 16.1% ± 5.3%, CD14⁺ DCs: 15.1% ± 17% ± 5.6%. (B) Allogeneic CFSE-labeled naive CD8⁺ T cells primed for 7 days by each dermal skin mDC subset were stained and analyzed by flow cytometry for the expression of granzyme B. The percentage of cells that diluted CFSE and expressed granzyme B is shown. One of 8 experiments is shown. (C) The plot shows the percentage of cells primed by each of the mDC subsets and expressed granzyme B (*n* = 8). (D) The plots show the expression of IFN-γ and TNF-α by naive CD8⁺ T cells that were primed by either dermal CD5⁺ or CD5⁻ DCs. CD8⁺ T cells primed by the dermal CD14⁺ DCs are shown as a control. One of 5 experiments is shown. (E) CFSE^{low}CD8⁺ T cells that were primed by either dermal CD1a^{dim}CD5⁺ or CD5⁻ DCs were reactivated by anti-CD3 and anti-CD28 mAbs for 18 hours. IFN-γ was measured in the culture supernatant by a Luminex magnetic bead assay. The graph shows the pooled results of 4 experiments. Data represent mean ± SEM; ***P* < 0.01, *****P* < 0.0001 by paired Student's *t* tests (A, C, and E).

Subsequently, the capacity of DCs to polarize CD4⁺ T cells was examined by measuring their cytokine production. Dermal CD5⁺ DCs induced a significant difference in the proportion of polarized IL-22-expressing T cells when compared with CD5⁻ DCs or those primed by CD14⁺ DCs (Figure 3, B and C). In addition, the amount of IL-22 produced by each T cell was higher in cells primed by dermal CD5⁺ DCs compared with those primed by dermal CD5⁻ DCs (Figure 3D, top). Although both CD5⁺ and CD5⁻ DCs could polarize IFN-γ-producing CD4⁺ T cells, CD5⁺ DCs were more efficient in this process (Figure 3, C and D, bottom).

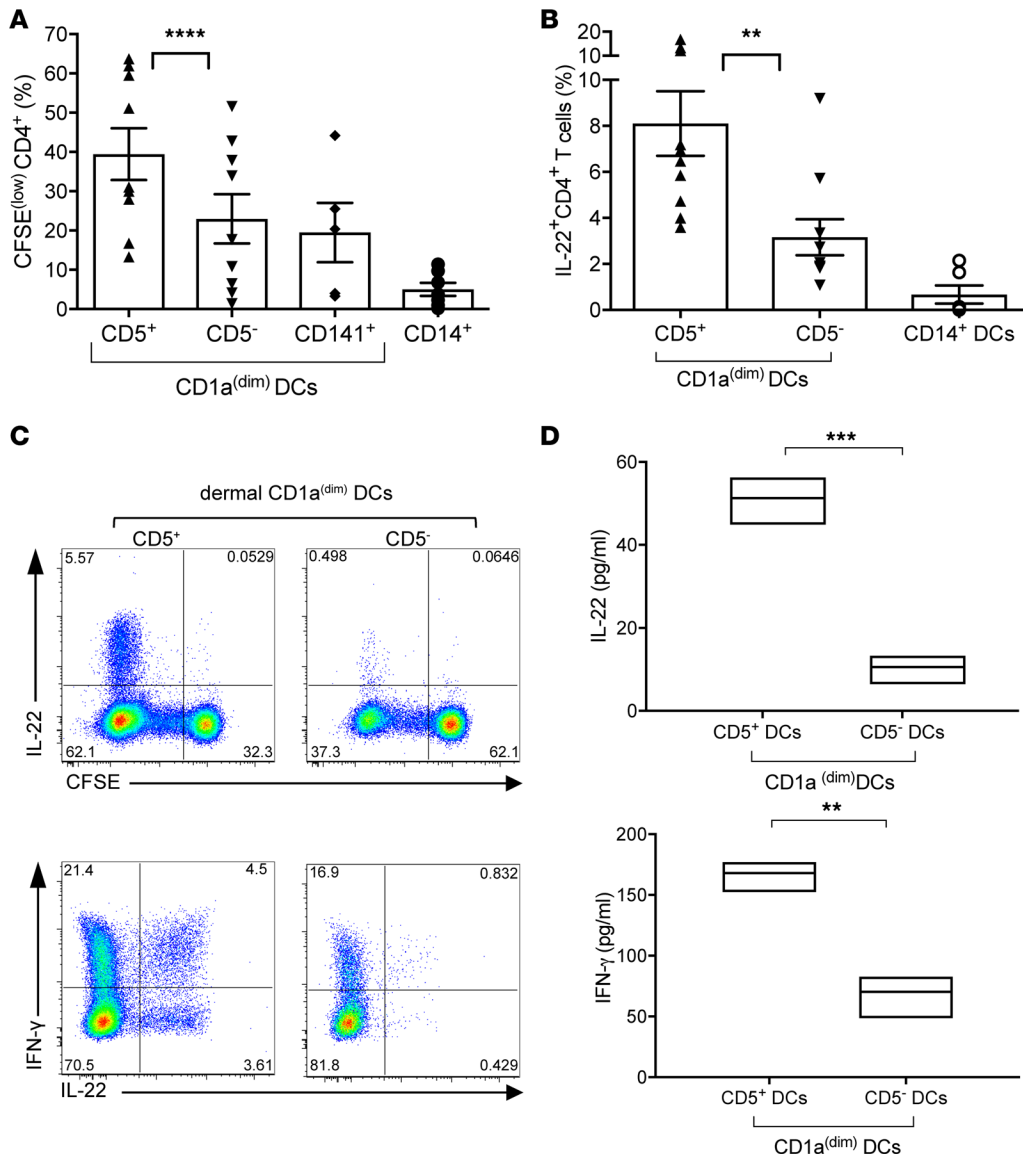


Figure 3. Dermal CD5⁺ DCs are superior to dermal CD5⁻ DCs at inducing the proliferation and differentiation of Th22 cells. (A) Proliferation of allogeneic naive CD4⁺ T cells primed with sorted CD40L-activated dermal CD5⁺ or CD5⁻ CD1a^{dim} DCs, dermal CD1a^{dim}CD141⁺, or dermal CD14⁺ DCs was measured after 7 days by CFSE dilution using flow cytometry. The graph shows the frequency of the CFSE^{low}CD3⁺CD4⁺ T cells (n = 10). Mean ± SD ± SEM for CD5⁺: 39.5% ± 19.8% ± 6.6%, CD5⁻: 22.9% ± 17% ± 7.6%, CD141⁺ DCs: 19.5% ± 17% ± 7.6%, CD14⁺ DCs: 5% ± 4.4% ± 1.65%. (B) CFSE-labeled sorted naive CD4⁺ T cells cultured for 6 days with CD40L-activated dermal CD1a^{dim}CD5⁺ or CD1a^{dim}CD5⁻ DCs. CFSE dilution and cytoplasmic expression of IFN-γ and IL-22 were analyzed by flow cytometry after 5-hour stimulation with PMA and ionomycin. (C) The plot shows the frequency of IL-22-producing CD4⁺ T cells that were primed by the different skin DC subsets (n = 10). Top: The plot shows the frequency CD4⁺ T cells that diluted CFSE and express IL-22. Bottom: The plot shows the frequency of IFN-γ and IL-22-producing CFSE^{low}CD4⁺ T cells. Data are representative of 7 independent experiments. (D) CFSE^{low}CD4⁺ T cells, primed by either dermal CD1a^{dim}CD5⁺ or CD5⁻ DCs, were sorted and restimulated with anti-CD3 and anti-CD28 mAbs for 18 hours. IL-22 and IFN-γ were measured by a Luminex multiplex bead assay (n = 3). One of 3 experiments is shown. Data represent mean ± SEM; **P < 0.01, ***P < 0.005, ****P < 0.0001 by paired Student's t tests (A and C) or unpaired Student's t tests (D).

Thus, dermal CD5⁺ DCs are more efficient than CD5⁻ DCs in inducing the proliferation and polarization of naive CD4⁺ T cells into IFN-γ and IL-22 cytokine-secreting cells.

Functional analysis of CD5⁺ and CD5⁻ LCs. Since we also found that a subset of LCs expressed CD5, we assessed their capacity to activate allogeneic naive CD8⁺ and CD4⁺ T cell responses. Live HLA-DR⁺CD1a^{hi}CD5⁺ and CD5⁻ LCs were cocultured with allogeneic naive T cells and analyzed after 7 days for T cell proliferation. Consistent with the findings obtained using dermal CD5⁺ and CD5⁻ DCs, we found that CD5⁺ LC subsets were more efficient than the CD5⁻ LCs at inducing allogeneic CD8⁺ T cell proliferation (Figure 4A). The number of granzyme B-producing primed CD8⁺ T cells (Figure 4, B and C), as well as

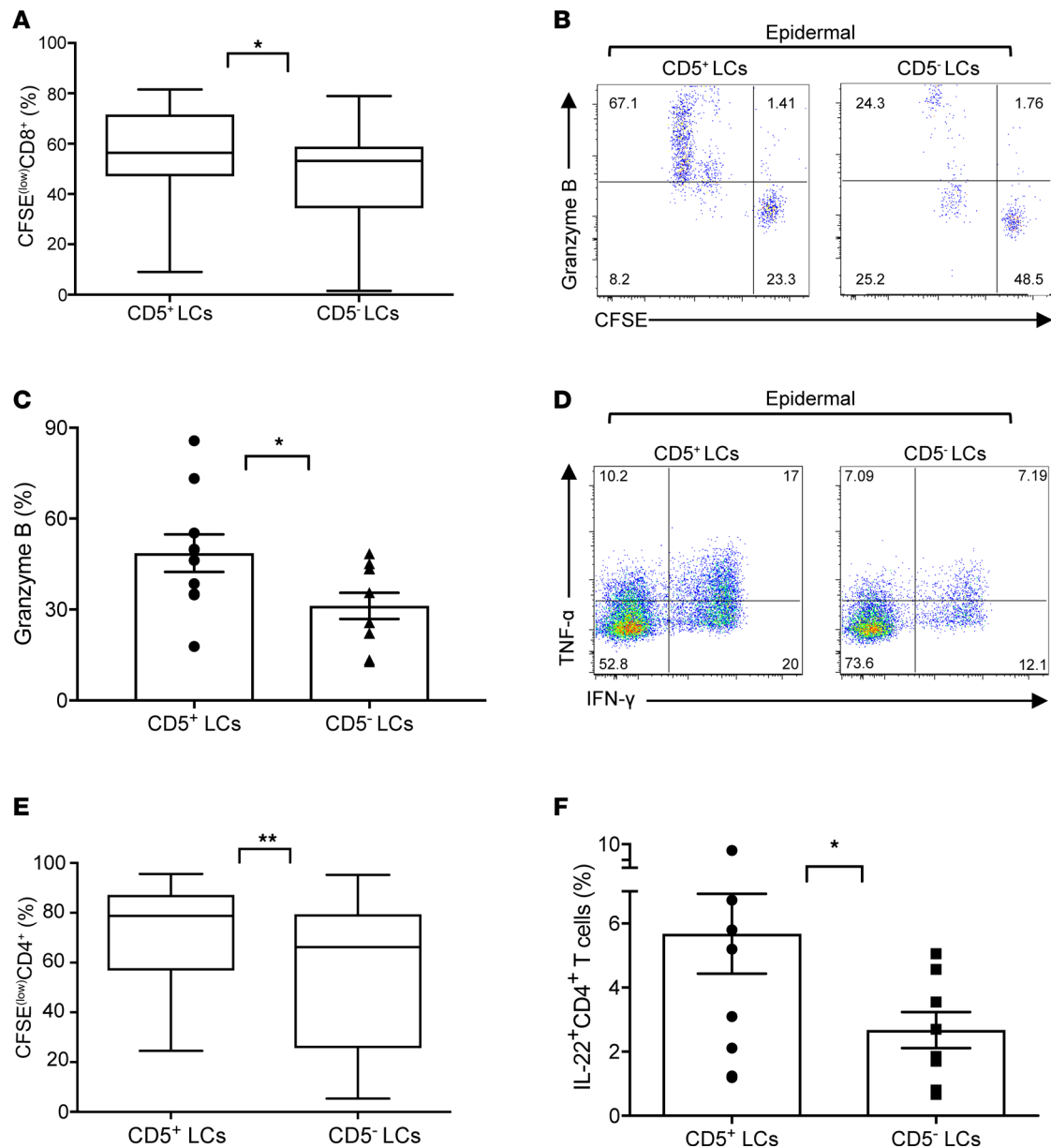


Figure 4. Functional characterization of CD5⁺ and CD5⁻ LC subsets. (A) The percentage of CFSE^{lo} allogeneic naive CD8⁺ T cells that were primed for 6–8 days by sorted activated CD5⁺ and CD5⁻ LCs. Results of 10 independent experiments are shown. Mean ± SD ± SEM CD5⁺ LCs: 56.4% ± 21.2% ± 6.7%; CD5⁻ LCs: 46.8% ± 20.1% ± 6.3%. (B) Allogeneic CFSE-labeled naive CD8⁺ T cells primed for 7 days by each LC subset were stained and analyzed by flow cytometry for the expression of granzyme B. The percentage of cells that diluted CFSE and expressed granzyme B is shown. One of 8 experiments is shown. (C) The plot shows the percentage of cells primed by each of the mDC subsets and expressed granzyme B ($n = 8$). (D) The plots show the expression of IFN- γ and TNF- α by naive CD8⁺ T cells that were primed by either CD5⁺ or CD5⁻ LCs. One of 3 experiments is shown. (E) The percentage of CFSE^{lo} allogeneic naive CD4⁺ T cells that were primed for 6–8 days by sorted activated CD5⁺ or CD5⁻ LCs ($n = 9$). Mean ± SD ± SEM CD5⁺ LCs: 71.7% ± 22.3% ± 7.4%; CD5⁻ LCs: 54.5% ± 31.4% ± 10.5%. (F) CFSE-labeled sorted naive CD4⁺ T cells cultured for 6 days with CD40L-activated CD5⁺ LCs or CD5⁻ LCs. The plot shows the frequency of IL-22-producing CD4⁺ T cells that were primed by the different LC subsets ($n = 10$). Data represent mean ± SEM; * $P < 0.05$ (A, C, and F), ** $P < 0.01$ (E) by paired Student's t tests.

the number of multifunctional IFN- γ - and TNF- α -producing CD8⁺ T cells (Figure 4D), was higher in cultures primed by the CD5⁺ LCs compared with the CD5⁻ LCs. We found that the CD5⁺ LC subset was also more efficient at inducing allogeneic CD4⁺ T cell proliferation than CD5⁻ LCs (Figure 4E) as well as in the differentiation of CD4⁺ T cells that produced IL-22 (Figure 4F). Overall, CD5 expression on LCs further potentiates their capacity to prime CTLs and Th22 cells.

CD5⁺ DCs are enriched in the epidermis and the dermis of psoriasis patients. Given the ability of skin CD5⁺ DCs to activate Th1 and Th22 cells, the hallmark response in the pathogenesis of psoriasis, we next assessed

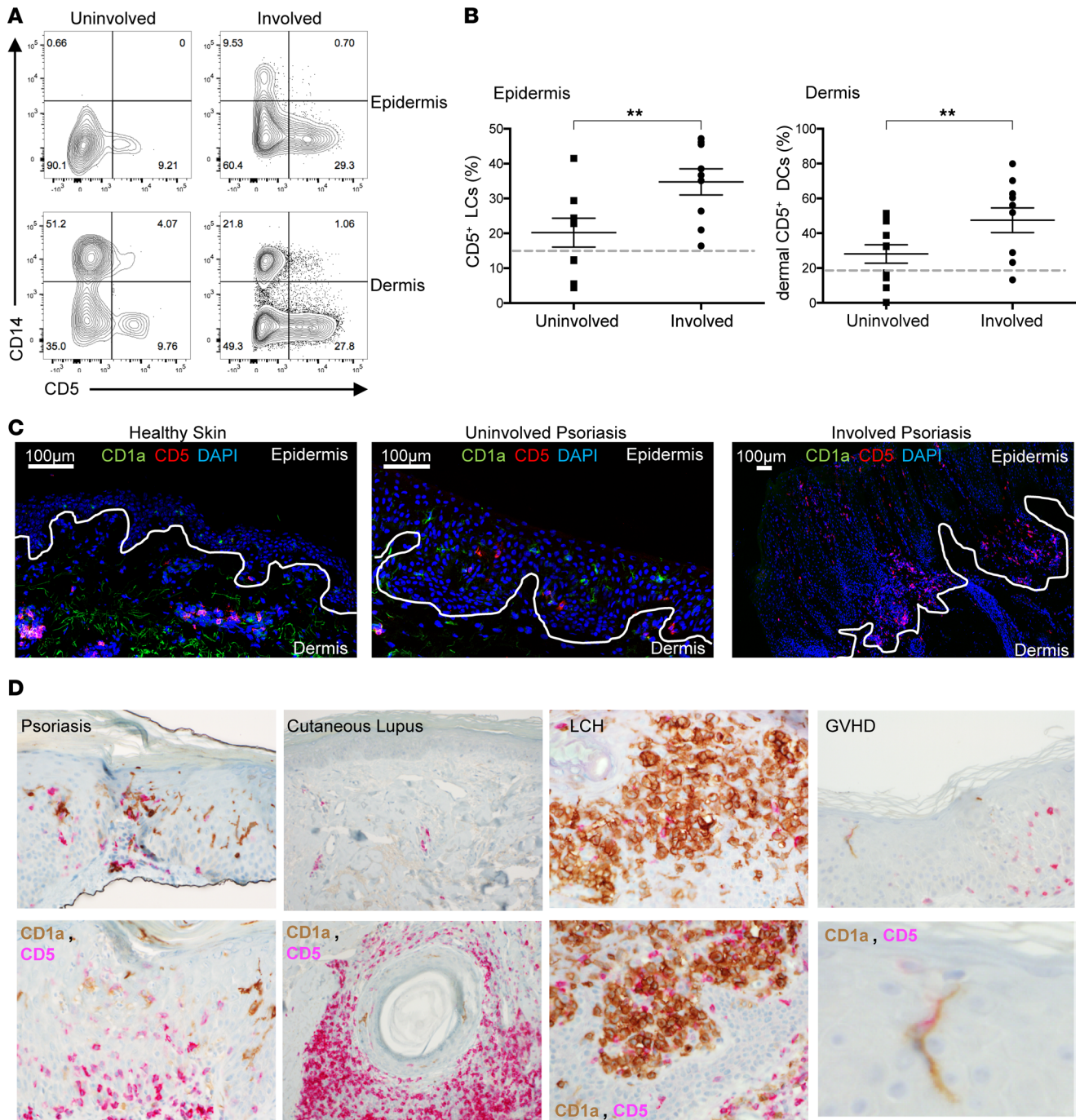


Figure 5. CD5⁺ LCs and dermal DCs are increased in psoriatic lesions compared with nonlesional psoriatic skin. (A) Expression of CD5 and CD14 on epidermal and dermal DCs from uninvolved (left arm) and involved (left forearm) lesions of psoriasis patient 025 (see Table 1). (B) The percentage of CD5⁺ DCs in the epidermis (left) and dermis (right) of uninvolved and involved skin lesions of 7 and 8 patients, respectively. The percentage of the total migrating DCs (HLA-DR⁺CD3/19/56⁻) cells. Mean ± SEM: epidermal CD5⁺ DCs, uninvolved, 23.4% ± 4.6%; involved, 35.7% ± 4.7%; dermal CD5⁺ DCs, uninvolved, 32.7% ± 5.2%; involved, 52.2% ± 7.8%. Dashed lines mark the levels of CD5⁺ DCs in healthy skin. Data represent mean ± SEM; ***P* < 0.01 by paired Student's *t* tests. (C) Immunofluorescence staining of CD5 and CD1a on healthy skin and psoriasis uninvolved and involved skin. Scale bar: 100 µM. (D) CD5 and CD1a expression in psoriasis, cutaneous lupus, Langerhans cell histiocytosis (LCH), and graft-versus-host diseased (GvHD) skin. Original magnification, ×20 (top); ×40 (bottom).

their involvement in the disease. Skin biopsies were obtained from involved psoriatic plaques and adjacent nonlesional skin (uninvolved) from patients with psoriasis. Dermal and epidermal DCs were purified in a similar manner to that with healthy skin and analyzed by flow cytometry. The frequency of CD5⁺ DCs in both the dermis and the epidermis was found to be 2-fold higher in the psoriatic skin plaque as compared

Table 1. Demographic data of psoriasis patients studied

Patient ID	Sex	Age	Involved tissue	Uninvolved tissue	Treatments (previous and current)	Type
PS001	Male	62	Unspecified	Unspecified	Unspecified	Plaque
PS004	Male	70	Buttock	Buttock	Unspecified	Plaque
PS005	Female	50	Left leg	Right arm	Humira, clobetasol ointment, methotrexate	Plaque
PS007	Female	76	Left buttock	Left back	Topical steroids and Enbrel	Plaque
PS011	Female	57	Right forearm	Right lower back	NBUVB, MTX, topicals, Humira, Taclonex	Plaque
PS012	Male	58	Right elbow	Right upper arm	NBUVB, Humira, MTX, clobetasol, triamcinolone	Plaque
PS013	Female	47	Right forearm	Left upper elbow	Triamcinolone	Plaque
PS016	Male	33	Left forearm	Left arm	Topical steroids	Plaque
PS017	Male	20	Right posterior medial leg	Right posterior lateral leg	Methotrexate, Humira	Chronic plaque and guttate
PS018	Female	76	Posterior neck	Right inner arm	Taclonex ointment (dexamethasone, Dovonex)	Plaque
PS019	Female	46	Right elbow	Right upper arm	Topical steroids and Enbrel	Plaque
PS025	Female	65	Left lateral lower leg		Topical steroids	Plaque
PS026	Female	80	Scalp and face		No previous treatment	Plaque

Psoriasis patient information, including sex, age, anatomical location of the involved and uninvolved biopsy specimens, treatment history, and type.

with the nonlesional skin in all patients examined (Figure 5, A and B). Interestingly, the uninvolved skin presented with higher amounts of CD5⁺ DCs compared with healthy skin by an average of 1.6 times (Figure 1B and Figure 5, B and C). The CD5⁺ DCs seen in the epidermis expressed lower amounts of CD1a (Supplemental Figure 2), suggesting that they might be newly differentiated bone marrow cells that migrated to the epidermis or dermal DCs that migrated to the epidermis. Increased numbers of CD5⁺ DCs, as measured by the coexpression of CD1a and CD5, were also observed in the epidermis and dermis in situ, using tissue immunostaining (Figure 5, C and D). In contrast with cutaneous lupus, in which high amounts of CD1a⁺CD5⁺ cells were found, and LC histiocytosis skin, which predominantly contained CD1a⁺CD5⁻ cells, skin of a graft-versus-host patient contained CD1a⁺CD5⁺ LCs, which were the only cell type detected in this patient (Figure 5D), suggesting their contribution to this inflammatory skin condition and consistent with the greater capacity of the CD5⁺ DCs to induce allogeneic CD8⁺ and CD4⁺ T cell responses (Figure 4, A and E). Overall, our data suggest that CD5⁺ DCs could play a key role in exacerbating the pathogenesis of psoriasis by promoting CTLs and inflammatory helper T cell responses.

CD34⁺ hematopoietic progenitors give rise to CD1c⁺CD5⁺ DCs. To define the developmental relationship between the CD5⁺ and the CD5⁻ subset, CD34⁺CD117⁺ hematopoietic progenitor cells (HPCs) from cord blood were differentiated into DCs on the mouse stromal cell line, MS-5, and in the presence of the cytokines, GM-CSF, stem cell factor (SCF), and FLT3 ligand (FLT3-L), as previously described (5, 26–28). The expression of CD5 was detected on the differentiated CD1c⁺ DCs after 7 days (Figure 6, A and B). These results were consistent with the characterization of skin DCs, in which the CD5⁺ DCs branch out as a subset of the CD1c⁺CD1a^{hi} DCs in the epidermis (LCs) and CD1c⁺CD1a^{dim} DCs in the dermis (ref. 5, Figure 1A, and Supplemental Figure 1A). CD11b expression was shared between the in vitro CD5⁺ DCs and dermal CD5⁺ DCs (Figure 1D). Langerin was only expressed on a small fraction of the in vitro CD1a⁺ DCs and by LCs (Figure 1D). In vitro CD5⁺ DCs expressed lower levels of the activation markers CD83, CD86, and CCR7 than skin DCs but higher levels than those expressed by blood CD5⁺ DCs (Figure 1D). Functionally, similar to their ex vivo counterparts, in vitro CD5⁺ DCs were also more efficient than the CD5⁻ DCs or CD14⁺ DCs at inducing the proliferation of allogeneic CD8⁺ T cells (Figure 6C) and priming CD8⁺ T cells to differentiate into CTLs that produced granzyme B and perforin (Figure 6D) as well as IFN- γ and TNF- α (Figure 6E). Moreover, CD5⁺ DCs that differentiated from CD34⁺ HPCs were more efficient than the CD5⁻ DCs or CD14⁺ DCs at inducing the proliferation of allogeneic CD4⁺ T cells and priming CD4⁺ T cells to differentiate into IL-22-producing cells (Figure 6, F and G). In addition, the amount of IL-22 produced per cell was higher in T cells that were primed by in vitro CD5⁺ DCs compared with those primed by in vitro CD5⁻ DCs (Figure 6H). Thus, CD5⁺ DCs develop from bone marrow independently of the CD5⁻ fraction and resemble their ex vivo counterparts.

TNF signaling enhances the development of CD5⁺ DCs from CD34⁺ hematopoietic progenitors. Next, we assessed whether the differentiation of CD5⁺ DCs would be altered in the presence of cytokines that are abundant in inflamed psoriatic skin, such as TNF- α and lymphotoxin α/β (LT α/β). Indeed, we found that addition of

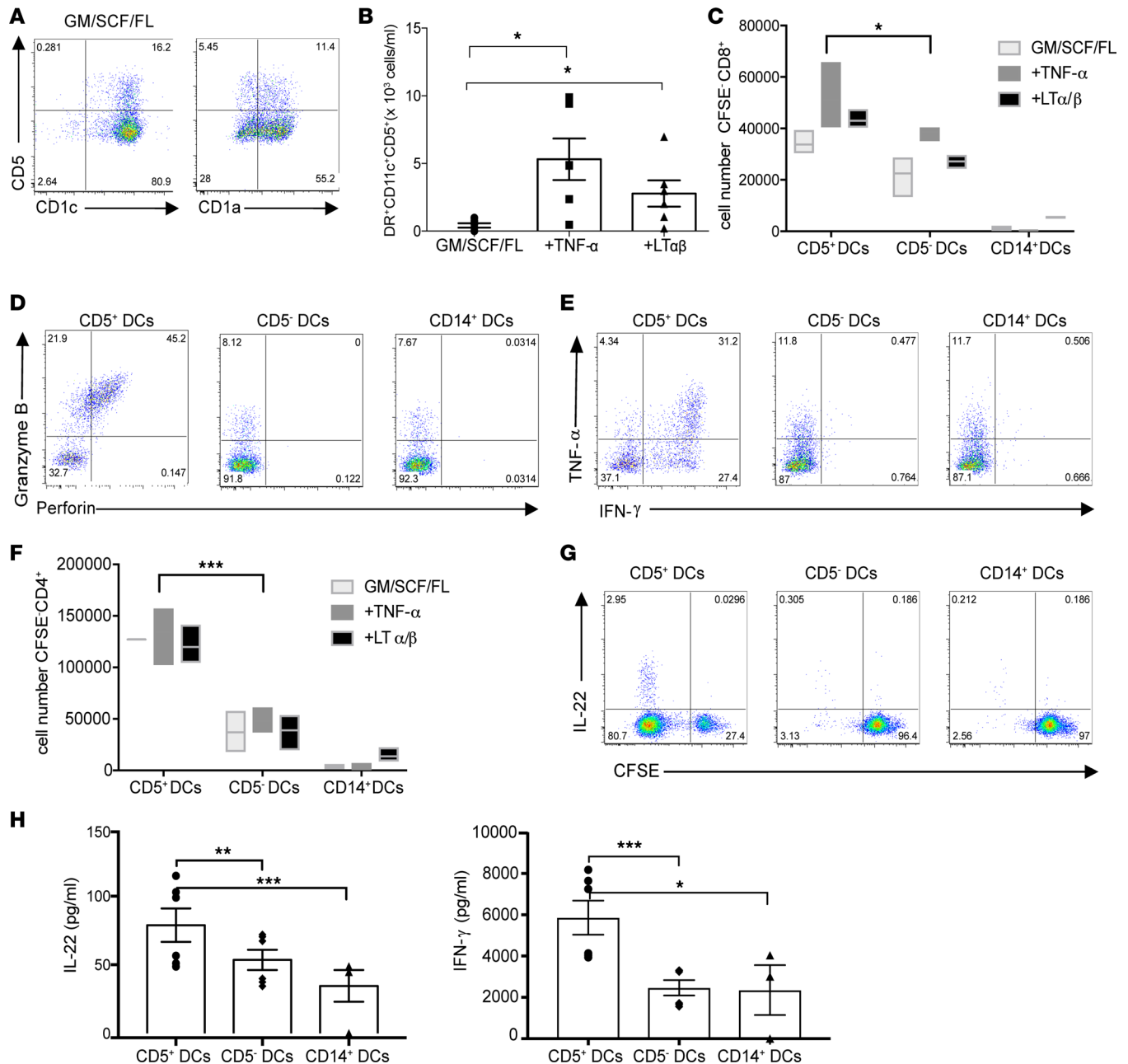


Figure 6. CD5 marks a functional terminally differentiated DC subset. (A) The plots show the frequency of CD11c⁺CD1a⁺CD5⁺ and CD11c⁺CD1c⁺CD5⁺ DCs obtained from cultures of cord blood CD34⁺CD117⁺CD123⁻ cells with GM-CSF (GM), SCF, and FLT3-L (FL) on day 7. (B) The graph shows the number of CD11c⁺CD1c⁺CD5⁺ DCs on day 7 of culturing CD34⁺ HPCs with indicated cytokines (*n* = 6). (C) Day 12 in vitro CD1c⁺CD5⁺, CD1c⁻CD5⁺, or CD14⁺ DCs were sorted and cocultured with naive T cells. The graph shows the number of CD8⁺ T cells that diluted CFSE in response to different DC subsets from the different culture conditions. (D) Sorted in vitro DC subsets were cocultured with naive allogeneic CFSE-labeled T cells for 7 days (300 DCs: 1 × 10⁵ T cells). CFSE^{lo} cells were analyzed for the expression of granzyme B and perforin. One of three experiments is shown. (E) Similar to D, the plot shows the expression of IFN- γ and TNF- α by naive CD8⁺ T cells that were primed by each in vitro DC subsets. One of 3 experiments is shown. (F) Similar to C, the graph shows the number of CD4⁺ T cells that diluted CFSE in response to different to different DC subsets from the different culture conditions. (G) Similar to D, the plot shows the fraction of CD4⁺ T cells that diluted CFSE and produced IL-22 following 6 days of priming with the different DCs subsets. One of 3 experiments is shown. (H) The plot shows IL-22 and IFN- γ production by CFSE^{lo}CD4⁺ T cells that were primed by each in vitro DC following reactivation by anti-CD3 and anti-CD28 mAbs for 18 hours (*n* = 6 for CD5⁺ and CD5⁻; *n* = 3 for CD14⁺ DCs). Data represent mean \pm SEM (B, C, F, and H); **P* < 0.05, ***P* < 0.01, ****P* < 0.005, *****P* < 0.0001 by paired Student's *t* tests.

TNF- α or LT α / β to GM-CSF, SCF, and FLT3-L promoted the differentiation of the CD11c⁺CD1c⁺CD5⁺ DCs (Figure 6B and Supplemental Figure 3B). The number of CD5⁺ DCs measured on day 7 increased from $0.42 \times 10^3 \pm 0.4 \times 10^3$ cells/ml with GM-CSF, SCF, and FLT3-L to $5.31 \times 10^3 \pm 3.7 \times 10^3$ cells/ml with addition of TNF- α and $2.78 \times 10^3 \pm 0.4 \times 10^3$ cells/ml with the addition of LT α / β (Figure 6B). The ability

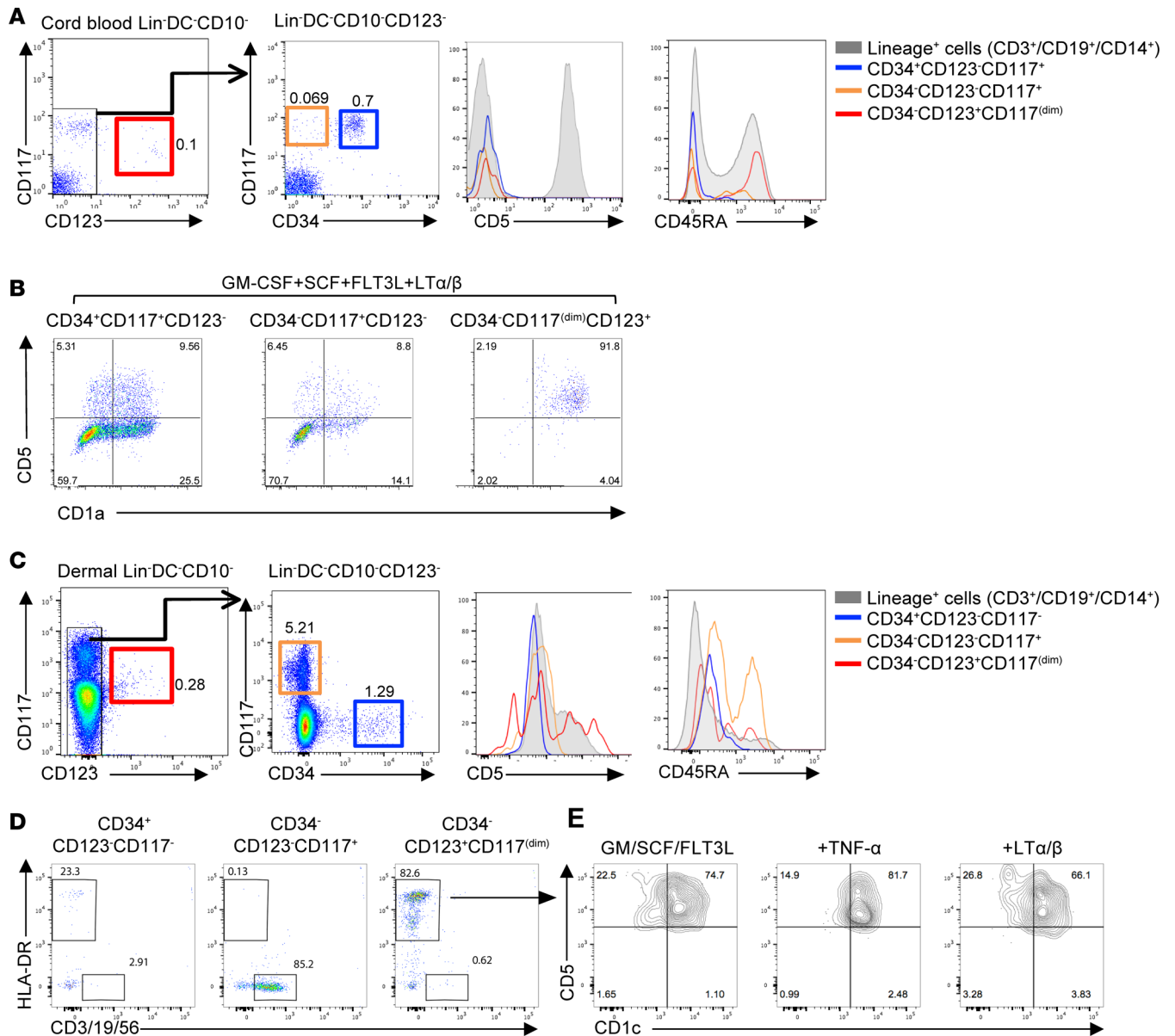


Figure 7. CD34⁺CD123⁺CD117^{dim}CD45RA⁺ cells preferentially give rise to CD5⁺ DCs. (A) Gating strategy for cord blood progenitors. Cells were sorted as Lin⁻DC⁻CD10⁻CD123⁻ (see also Supplemental Figure 3): CD34⁺CD117⁻ (blue); CD34⁺CD117⁺ (orange); or Lin⁻DC⁻CD10⁻CD123⁻CD34⁻CD117^{dim}CD45RA⁺ (red). Histograms show the expression of CD5 and CD45RA on the different progenitor subsets. Expression on lineage⁺ cells is shown as a control (gray). (B) Sorted cord blood CD34⁺CD123⁻CD117⁻, CD34⁺CD123⁻CD117⁺, or CD34⁻CD123⁺CD117^{dim} progenitors were cultured in the presence of GM-CSF, SCF, FLT3-L, and LTα/β. Flow cytometry plots, gated on live CD45⁺HLA-DR⁺CD11c⁺ cells, show culture output of CD1a⁺CD5⁺ DCs on day 7. Representative results of 4 independent experiments are shown. (C) Gating strategy for dermal progenitors. Cells were sorted as Lin⁻DC⁻CD10⁻ that were CD34⁺CD123⁻CD117⁻ (blue); CD34⁺CD123⁻CD117⁺ (orange); or CD34⁺CD123⁺CD117^{dim} (red). Histograms show the expression of CD5 and CD45RA on the different progenitor subsets. (D) CD34⁺CD123⁻CD117⁻, CD34⁺CD123⁻CD117⁺, or CD34⁺CD123⁺CD117^{dim} were isolated from human dermis. Flow cytometry plots are gated on live CD45⁺HLA-DR⁺CD11c⁺ cells and show the expression of HLA-DR⁺ or lineage⁺ cells that were differentiated from the different progenitors. (E) The plots show the expression of CD1c and CD5 on HLA-DR⁺ cells that differentiated from CD34⁺CD123⁺CD117^{dim} cells for 7 days in the presence of in the presence of GM-CSF (GM), SCF, and FLT3-L (FL) and either TNF-α or LTα/β. Representative results of 3 independent experiments are shown.

of the CD5⁺ DCs to expand allogeneic CD4⁺ and CD8⁺ T cells was higher than that of CD5⁻ DCs and CD14⁺ DCs, regardless of whether the cells were cultured in the presence of TNF-α or LTα/β (Figure 6, C and F). Overall, CD5⁺ DCs branch out from the CD1c⁺ DCs and their differentiation potential is enhanced by TNF-α signaling, including TNF-α and LTα/β.

CD34⁺CD123⁺CD117^{dim}CD45RA⁺ cells are an immediate precursor to human CD5⁺ DCs. The fact that only a fraction of CD34⁺ HPCs differentiated into CD5⁺ DCs led us to hypothesize that a committed progenitor

for CD5⁺ DCs might exist in the bone marrow. Thus, we assessed whether CD5⁺ DCs would differentiate from the recently identified DC precursors (pre-cDC), CD34⁻ progenitors (27, 28). Progenitors were sorted from cord blood as lineage⁻(CD3/19/56/14/66b)DC⁻(CD1c/141/303)CD10⁻CD123⁻ cells that were either CD34⁺CD117⁺ (GMDPs/MDPs) or CD34⁻CD117⁺ (pre-cDC) (Figure 7A) and cultured for 7 days on MS-5 cells with GM-CSF, SCF, FLT3-L, and LT α / β . Indeed, both CD11c⁺CD1a⁺CD5⁺ and the CD11c⁺CD1a⁺CD5⁻ DCs differentiated from the CD34⁺CD117⁺ or the CD34⁻CD117⁺ DC progenitors (Figure 7B). We noticed, however, a third progenitor population within the CD34⁻ lineage(CD3/19/56/14/66b)DC(CD1c/141/303)CD10⁻ population that was marked by CD123⁺ and low levels of CD117 and expressed CD45RA (Figure 7A, red). Surprisingly, we found that under similar culture conditions, these cells preferentially differentiated into CD11c⁺CD1a⁺CD5⁺ DCs (Figure 7B). Thus, the high clonal efficiency and differentiation potential of the CD34⁻CD123⁺CD117^{dim}CD45RA⁺ progenitor cell suggests that it could represent a committed progenitor for the CD5⁺ DCs.

CD34⁻CD123⁺CD117^{dim} progenitors are found in human dermis and give rise to CD5⁺ DCs. We next assessed whether this progenitor population is present in skin. Thus, cells were isolated from epidermis and dermis and analyzed for the presence of progenitors in a similar manner to the cord blood within the lineage(CD3/19/56/14/66b)DC(CD1c/141/303)CD10⁻ population. Within the CD123⁻ fraction of the dermis, but not epidermis, we found a population of CD34⁺ HPCs as well as CD34⁻CD117⁺ cells. However, in contrast with cord blood, dermal CD34⁺ cells did not express CD117 (Figure 7, A and C, blue gate).

Similar to cord blood, we found a population marked by CD123 that expressed low levels of CD117 (Figure 7C, red gate); however, compared with the cord blood CD123⁺ progenitors, which were negative for CD5 and expressed CD45RA (Figure 7A, red histograms), the dermal CD123⁺ population expressed low levels of CD5 and lower levels of CD45RA (Figure 7C, red histograms). Sorted progenitors were cultured on mouse stromal cells in the presence of cytokines for 7 days. As shown in Figure 7D, dermal CD34⁺ HPCs gave rise to 20% HLA-DR⁺ cells and 2% lymphoid cells (CD3/CD19/CD56), and dermal CD34⁻CD123⁻CD117⁺ gave rise primarily to lymphoid cells (85.2%). The CD34⁻CD123⁺CD117^{dim} HPCs gave rise primarily to HLA-DR⁺ cells (82.6%), and the majority of these cells expressed CD1c and CD5 (Figure 7E). The differentiation of the CD1c⁺CD5⁺ DCs occurred in the presence or absence of LT α / β or TNF- α (Figure 7E). Thus, a progenitor for the CD1c⁺CD5⁺ DCs is present in human dermis.

Discussion

Here, we have further unraveled the complexity of the human skin DC system and its progenitor cells in the dermis. We show that CD5 marks a terminally differentiated inflammatory DC subset. Its presence in the epidermis highlights a previously unappreciated heterogeneity within human LCs, which has been previously noted in the mouse (29). The presence of the CD5⁺ DCs at early stages of the immune system development, i.e., in cord blood, which has never been exposed to a foreign antigen, further supports our hypothesis that CD5 demarks what we believe to be a unique subset rather than an activation state.

In addition to elevated levels of the inflammatory CD5⁺ DCs in psoriatic plaques, we also observed that CD5⁺ LCs (as detected by the expression of CD5 and CD1a) were the only epidermal DCs in acute graft-versus-host disease patient skin, suggesting their involvement in both of these inflammatory diseases. Indeed, genome-wide association studies revealed a pathogenic relevance for CD5 in inflammatory bowel disease (IBD) (30), multiple sclerosis (31), and rheumatoid arthritis (RA) (32). Similar to psoriasis, Th22 cells and plasma IL-22 levels play a detrimental role in RA. Since CD5⁺ DCs are potent activators of Th22 response, a therapy that specifically targets CD5⁺ DCs to prevent Th22 cell induction and reduce IL-22 levels might ameliorate symptoms of both of these diseases (33). On the other hand, IL-22 plays crucial roles in regulating barrier immunity and antimicrobiota (34) and can potentially protect patients with ulcerative colitis (UC), a form of IBD in which IL-22-producing cells are reduced in the gut (35). Therefore, harnessing CD5⁺ DCs to restore Th22 cells to the intestinal mucosa during active inflammation may be an avenue for novel therapeutics against UC. Interestingly, Crohn's disease, which is another form of IBD, is characterized by elevated levels of Th17 cytokines (IL-17 and IL-22); this points to the possibility that CD5⁺ DCs could serve as a biomarker to distinguish between these two very different forms of IBD. Future studies will be important to understand the role of CD5 on DCs in these pathological conditions.

Several possible mechanisms might account for the ability of CD5 on DCs in mediating these robust T cell responses. Although there is no confirmed ligand for CD5, a recent study suggests that CD5 may be homophilic, binding CD5 on the surface of other cells (36). In addition, it was also shown that the ligation

of CD5 on T cells results in the polarization of naive T cells into the Th17 pathway (37), and, more recently, in the mouse, a CD5-like molecule (CD5L) was shown to regulate the pathogenicity of Th17 (38, 39). Thus, we surmised that CD5 on DCs might bind to CD5 (or CD5L) on T cells, resulting in effector T cell polarization. Initial assessment of the role of CD5 costimulation on DCs by using a monoclonal antibody to CD5 during a coculture led to increased T cell activation, suggesting that ligation of CD5 on DCs may deliver a positive signal or promote their activation. Interestingly, a study that was relatively overlooked showed that CD5 recognizes the fungal cell wall component, zymosan (40). Thus, it is also possible that CD5 expression on DCs serves as a pattern recognition receptor and mediates the production of proinflammatory cytokines upon activation. This is intriguing, as none of the other known receptors for zymosan (i.e., TLR-2 or dectin-1) are present on CD5⁺ LCs and dermal CD1a^{dim}CD5⁺ DCs; however, they are highly abundant on the dermal CD14⁺ DCs (25). Whether CD5 recognizes other pathogen-associated molecular patterns besides zymosan remains to be established. Overall, the rapid proliferation and T cell differentiation mediated by CD5⁺ DCs led us to propose that these DCs may be prone to respond faster to a foreign antigen and that CD5 might facilitate the recognition of a danger signal. If this hypothesis is true, this functionality of the CD5⁺ DCs could be advantageous, particularly in the skin, which serves as the first line of defense against pathogens. Moreover, as a scavenger receptor, CD5 may plausibly serve as an uptake or a pathogen clearance receptor to mediate cross-presentation of dead cell-associated proteins by DCs and activation of antigen-specific CD8⁺ T cells, similar to Clec9A (41, 42), which has restricted expression to CD141⁺ DCs in humans. In addition, since CD5 expression is restricted to the CD1a⁺CD1c⁺ DCs, it might even mediate the presentation of lipids onto nonclassical MHC class I and the priming of CD1a-restricted Th22, as seen in patients with psoriasis (14, 43).

We have noticed that the differences between the dermal CD5⁺ and the CD5⁻ DCs in priming allogeneic T cell responses (Figure 2A and Figure 3A) were greater than those between CD5⁺ LCs and CD5⁻ LCs (Figure 4, A and E). As previously reported, LCs are highly effective initiators of allogeneic T cell responses (5, 9, 44) and thus, limiting culture conditions (i.e., high DC/T cell ratio, low IL-2) permitted us to reveal the contribution of CD5 to the outcome of the T cell responses. We envision that CD5⁺ LCs will be particularly efficient at priming an antigen-specific response where the T cell precursor frequency is low or when the antigen is of low affinity, like those that are expressed in tumors.

The developmental stages of human DCs are still incompletely defined. We show that, once differentiated, dermal CD1c⁺CD5⁻ DCs (Figure 1E), but also CD5⁻ LCs (data not shown), would not upregulate CD5 upon activation, suggesting that CD5 does not represent an activation marker. Our tested DC activators in this assay, however, do not exhaust the possibility that within the skin microenvironment, in response to a pathogen or a chronic condition, CD5 expression could be modulated on the DCs. Nevertheless, the presence of CD5⁺ DCs in cord blood (Supplemental Figure 1A), which has never been exposed to a foreign antigen, further supports our hypothesis that CD5 demarked a unique subset. We show that CD5⁺ DCs can be differentiated from human CD34⁺ HPCs isolated from cord blood and from a pre-cDC progenitors CD34⁺CD117⁺ cells (26). The differentiated CD5⁺ cells represented a subset of the CD1a⁺CD1c⁺ DCs and the CD1a^{dim} or ^{neg}CD1c⁺ DCs. The former may be similar to the CD1a^{hi}CD1c⁺CD5⁺ LCs, while the latter may be similar to the blood CD1c⁺ DCs and to the dermal CD1a^{dim}CD1c⁺ DCs. Consistent with our findings, FLT3 was shown in patients to induce the generation of CD5-expressing blood DCs (45), and functionally, the CD1c⁺CD5⁺ DCs in the blood appear to share the superior capacity for enhancing CD4⁺ T cell proliferation (46), as we found with the skin and in vitro-differentiated CD5⁺ DCs. Our study identified a progenitor marked as CD34⁺CD123⁺ cells in cord blood and in human dermis that gave rise primarily to the CD11c⁺CD1c⁺CD5⁺ DCs, which we referred to as “pre-CD5⁺ DCs.” Pre-cDCs were initially found in humans within the CD34⁺CD123⁻ fractions (28); however, a recent study reported the presence of CD123^{hi}CD33⁺CD45RA⁺CD303⁺ pre-DCs in peripheral blood (47). In contrast with See et al., our gating strategy excluded all the cells that expressed the pDC marker CD303/B220-2; thus, perhaps we looked at a distinct, possibly more committed, pre-cDC subset. Whether the CD123^{hi}CD33⁺CD45RA⁺ precursors identified in that study can be differentiated into CD5⁺ DCs was not tested; however, they were reported to express CD5. Two additional studies identified CD123⁺ DC populations in peripheral blood that are within the pDC gate and also express CD5, one that is a subset of pDC (48) and the other referred to as “AS DCs,” expressing Axl and Siglec6 (49). The latter were able to transition toward the CD1c⁺ DC state in vitro with superior capacity to activate T cells; however, the authors claim that these cells are less likely to be progenitors. Single-cell profiling studies are needed to determine whether and how these CD123⁺ precursors and CD123⁺ DCs are related.

We found that TNF-R signaling (including TNF- α and LT α / β) promoted the differentiation of uncommitted pre-DCs into CD1c⁺CD5⁺ DCs. In the mouse, lymphotoxin- β receptor signaling was required for the differentiation step of a subset of the CD11b⁺ DCs expressing high amounts of ESAM (50). Interestingly, blood CD1c⁺CD5⁺ DCs were recently shown to share a genetic signature with the ESAM^{hi} mouse DC population (46). Thus, conceivably, exposure of dermal progenitors (CD123⁺CD117^{dim}) to LT α / β in the skin might make them prone to develop into the CD5⁺ DC subset, rendering them a potent source of inflammatory CD5⁺ DCs, ready for rapid mobilization and T cell activation. However, unabated induction of CD5⁺ DCs from dermal progenitors by excess amounts of TNF- α and LT α / β may drive the autoimmune response in psoriasis. Ultimately, defining the mechanisms that maintain these cells in their initial uncommitted state in health and disease could lead to the development of new therapeutic strategies to modulate this differentiation process.

We were limited from using a mouse model for psoriatic disease in this study due to the global expression of CD5 in the mouse. CD5 is expressed on lymphocytes and DCs; thus, a global knockout for CD5 would not provide a definitive answer for the role of CD5 expression on each cell type in the disease. Future studies should attempt to generate a mouse with a specific deletion of CD5 on DCs to be used in a disease model. Furthermore, it is not known whether the function of mouse and human CD5⁺ DCs is similar. A recent study by Artyomov and Munk et al. (25) showed that human and mouse DCs that are similar anatomically and, in fact, may have different functions. This may add to the complexity of studying a disease such as psoriasis, which is only transient in current rodent models but chronically affects millions of humans.

Overall, we envision that mobilization of CD5⁺ DCs will be beneficial in vaccination where CTL induction is desired, such as in cancer. On the other hand, strategies to regulate CD5⁺ DC composition or function will represent an innovative approach for the treatment of psoriasis and other immune-mediated disorders in and beyond the skin.

Methods

Skin and blood specimens. Healthy human skin was obtained from donors who underwent cosmetic and plastic surgeries at Washington University School of Medicine in St. Louis and Barnes-Jewish Hospital (St. Louis, Missouri, USA) in accordance with institutional review board guidelines. Psoriatic plaque biopsy samples or whole-blood samples were acquired at Barnes-Jewish West County Hospital (St. Louis, Missouri, USA) in accordance with institutional review board guidelines. Lupus, LC histiocytosis, and graft-versus-host disease skin specimens were obtained from the Dermatopathology Center at Washington University School of Medicine in St. Louis. Patient and specimen characteristics are listed in Table 1.

DC isolation. Skin DC subsets were isolated as described previously (5). Briefly, tissue specimens were incubated with the bacterial protease, Dispase type II (Roche), for 18 hours at 4°C. Epidermal and dermal sheets were then separated and placed in RPMI 1640 (Gibco) supplemented with 10% fetal bovine serum (GemCell) and incubated for 48 hours at 37°C. The cells that migrated into the medium were enriched using a Ficoll-diatrizoate gradient, Lymphocyte Separation Medium (MP Biomedicals). DCs were stained using the antibodies listed in Supplemental Table 1 and were further purified by cell sorting using a BD FACSAria II. HLA-DR⁺CD3⁻CD19⁻ DCs subsets are marked in the epidermis as CD1a^{hi}Langerin⁺CD5⁺ or CD1a^{hi}Langerin⁺CD5⁻. In the dermis, the four DC subsets are marked as CD1a^{dim}CD141⁻CD5⁺, CD1a^{dim}CD141⁻CD5⁻, CD1a^{dim}CD141⁺, or CD14⁺ DCs. CD40L (100 ng/ml; R&D Systems) was used to activate DCs. The stability of CD5 expression on skin DCs was assessed by culturing sorted CD5⁺ or CD5⁻ DCs from the dermis with indicated DC activators for a period of 6 days. The expression of CD5 was analyzed by flow cytometry.

Human CD34⁺ HPCs and CD34⁻ pre-DCs isolation and differentiation. Cord blood samples were purchased from the St. Louis Cord Blood Bank and processed according to protocols approved by the Institutional Review Board at the Washington University School of Medicine in St. Louis. Immediately upon sample arrival, the cord blood was incubated with RosetteSep Human Hematopoietic Progenitor Cells Enrichment Cocktail (StemCell) to deplete CD2, CD3, CD14, CD16, CD19, CD24, CD56, CD61, and CD66b from the cord blood. Further, mononuclear cells were isolated by Ficoll-diatrizoate density gradient centrifugation, using Ficoll-Paque PLUS (GE Healthcare Life Sciences) at 800 g, for 30 minutes. CD34⁺ HPCs were isolated from cord blood mononuclear cells through positive selection using the EasySep Human CD34 Positive Selection Kit (StemCell Technologies) or

Miltenyi Biotec CD34⁺ microbeads or were labeled with an antibody mix (Supplemental Table 1) and sorted using a BD AriaII. Cord blood progenitor cells were sorted as live Lin⁻(CD1c, CD141, BDCA2)⁻CD10⁻ that were also CD34⁺CD123⁻CD117⁺, CD34⁻CD123⁻CD117⁺, or CD34⁻CD123⁺CD117^{dim}CD45RA⁺. Dermal progenitor cells were sorted as live Lin⁻(CD1c, CD141, BDCA2)⁻CD10⁻ that were also CD34⁺CD123⁻CD117⁻, CD34⁻CD123⁻CD117⁺, or CD34⁻CD123⁺CD117^{dim}. Progenitors were cultured as described previously (26). Briefly, MS-5 stromal cells (a gift from Kang Liu, Columbia University, New York, New York, USA) were maintained in complete α -Minimum Essential Medium (α MEM) media supplemented with L-glutamine, but without ribonucleosides and deoxyribonucleosides (Invitrogen) and with 10% heat-inactivated fetal calf serum (GemCell) and 1% penicillin/streptomycin (Invitrogen). 24 hours prior to coculture with HPCs, stromal cells were treated with 10 μ g/ml Mitomycin C (Sigma-Aldrich) for 3 hours at 37°C and plated at 2.5×10^4 cells per 100 μ l in a 96-well flat-bottom plate. 1×10^3 to 1×10^4 HPCs and cytokines were added in 100 μ l supplemented α MEM. FLT3-L (R&D Systems) was used at 200 ng/ml, SCF (R&D Systems) at 40 ng/ml, GM-CSF (Sanofi) at 50 ng/ml, TNF- α (R&D Systems) at 10 ng/ml, and LT α 1/ β 2 (Sigma-Aldrich) at 50 ng/ml. Cells were cultured for 5–10 days. All cytokines were replenished in full dose on day 5 except for FLT3-L, which was used at 100 ng/ml for replenishment.

Immunofluorescence analysis of CD5 expression. Healthy skin and formalin-fixed psoriasis biopsy specimens from lesional (involved) and adjacent nonlesional skin (uninvolved) were embedded in OCT for immunofluorescence staining. Tissue sections were cut into 10- μ m sections using the Leica CM 1950. Sections were fixed in 4% PFA for 15 minutes at room temperature and washed with PBS containing 3% bovine serum albumin (BSA) and 10% saponin. The sections were then quenched with 0.5 M glycine for 5 minutes, washed, and blocked with PBS/BSA/saponin for 30 minutes at room temperature. Sections were stained overnight with monoclonal mouse anti-human CD5 (5 μ g/ml; UCHT2, eBioscience) or isotype controls, washed, and incubated with anti-mouse Cy3 (3 μ g/ml, Jackson ImmunoResearch) for 2 hours. Samples were then washed and stained with mouse anti-human CD1a-FITC (100 mg/ml; NA1/34, DAKO) for 2 hours followed by DAPI for 20 minutes at room temperature. Tissue sections were mounted (ProLong mounting medium, Invitrogen). Images were acquired using an Olympus Confocal Microscope FV1000 using Fluoview software. Image analysis was performed using ImageJ software (NIH).

DC and T cell cocultures. Naive T cells were isolated using a Pan Naive T cell isolation kit (Miltenyi Biotec) according to the manufacturer's protocol or stained and sorted as CCR7⁺CD45RA⁺CD8⁺ or CCR7⁺CD45RA⁺CD4⁺ cells (See Supplemental Table 1). Isolated T cells were labeled with 0.5 μ M CFSE dye from the CellTrace CFSE cell proliferation kit (Invitrogen), according to the manufacturer's protocol. The CFSE-labeled T cells were then cultured with sorted skin DCs for 7–10 days. Proliferation was assessed by the percentage of CFSE-labeling dilution. IL-22, IFN- γ , and granzyme B production were assessed by flow cytometry after a short restimulation with PMA (Sigma-Aldrich; 25 ng/ml) and Ionomycin (Sigma-Aldrich; 1 μ M). Alternatively, proliferated cells marked as CFSE⁰, which constitute anything beyond one division (Supplemental Figure 4), were sorted and stimulated overnight with anti-CD3 and anti-CD28 mAbs (DYNAL 8 $\times 10^5$ beads per 3×10^5 cells). Cytokines produced by the cells were assessed in the supernatant using a Luminex multiplex bead assay.

Microscopy. Sorted skin DCs were cytospun and stained with Wright-Giemsa stain using a Hema 3 kit (Fisher Scientific). Images were acquired using a Leica $\times 63/1.40$ oil objective on a Leica DMIRB microscope with a Leica DFC310 FX camera.

Statistics. Statistical analysis was done using 2-tailed *t* test. Significance was defined as $P < 0.05$.

Study approval. The present studies were reviewed and approved by the Washington University School of Medicine in St. Louis Institutional Review Board. Written informed consent was received from each participant prior to collection of psoriatic skin biopsies or blood.

Author contributions

DK and LG conducted experiments, analyzed data, and reviewed and edited the manuscript. AM, JM, and AS conducted experiments and analyzed data. TT provided healthy human skin specimens. CM provided psoriasis patient specimens and clinical data. EK conceived and designed the study, performed and supervised experiments and data analysis, and wrote the manuscript.

Acknowledgments

We thank Erica Maria Lantelme, Marina Cella, Dorjan Brinja, and Emily Mannin at the Washington University School of Medicine in St. Louis Department of Pathology and Immunology for their help; Lisa Wu for help with editing this manuscript; and Kang Liu for providing the MS-5 cell line. We thank the surgeons, nurses, and staff at Barnes-Jewish Hospital and the Washington University School of Medicine in St. Louis Department of Surgery for providing access to skin samples. We thank Paul Allen, Gwendalyn Randolph, and Andrey Shaw for their advice and critical reading of the manuscript. This work was supported by funding from the Washington University School of Medicine in St. Louis Department of Pathology and Immunology and the Siteman Cancer Center to EK. This work was presented at the CIML 40th anniversary conference in Marseille, France, in September 2016; at the Aegean International Conference on Human & Translational Immunology in Rhodes, Greece, in September 2016 (51); at the 14th International Symposium on Dendritic Cells in Shanghai, China, in October 2016; and at the Inflammatory Skin Disease Summit — The Translational Revolution, The New York Academy of Medicine, in New York, New York, USA, in November 2016.

Address correspondence to: Eynav Klechevsky, Washington University School of Medicine, Department of Pathology and Immunology, 425 South Euclid, Saint Louis, Missouri 63110, USA. Phone: 314.286.0897; Email: eklechevsky@wustl.edu.

1. Banchereau J, Steinman RM. Dendritic cells and the control of immunity. *Nature*. 1998;392(6673):245–252.
2. Klechevsky E. Functional diversity of human dendritic cells. *Adv Exp Med Biol*. 2015;850:43–54.
3. Klechevsky E. Human dendritic cells — stars in the skin. *Eur J Immunol*. 2013;43(12):3147–3155.
4. Lenz A, Heine M, Schuler G, Romani N. Human and murine dermis contain dendritic cells. Isolation by means of a novel method and phenotypical and functional characterization. *J Clin Invest*. 1993;92(6):2587–2596.
5. Klechevsky E, et al. Functional specializations of human epidermal Langerhans cells and CD14⁺ dermal dendritic cells. *Immunity*. 2008;29(3):497–510.
6. Caux C, et al. CD34⁺ hematopoietic progenitors from human cord blood differentiate along two independent dendritic cell pathways in response to granulocyte-macrophage colony-stimulating factor plus tumor necrosis factor alpha: II. Functional analysis. *Blood*. 1997;90(4):1458–1470.
7. Caux C, et al. CD34⁺ hematopoietic progenitors from human cord blood differentiate along two independent dendritic cell pathways in response to GM-CSF+ TNF- α . *J Exp Med*. 1996;184(2):695–706.
8. Chu CC, et al. Resident CD141 (BDCA3)+ dendritic cells in human skin produce IL-10 and induce regulatory T cells that suppress skin inflammation. *J Exp Med*. 2012;209(5):935–945.
9. Banchereau J, et al. The differential production of cytokines by human Langerhans cells and dermal CD14(+) DCs controls CTL priming. *Blood*. 2012;119(24):5742–5749.
10. Banchereau J, et al. Immunoglobulin-like transcript receptors on human dermal CD14⁺ dendritic cells act as a CD8-antagonist to control cytotoxic T cell priming. *Proc Natl Acad Sci U S A*. 2012;109(46):18885–18890.
11. Seneschal J, Clark RA, Gehad A, Baecher-Allan CM, Kupper TS. Human epidermal Langerhans cells maintain immune homeostasis in skin by activating skin resident regulatory T cells. *Immunity*. 2012;36(5):873–884.
12. Penel-Sotirakis K, Simonazzi E, Péguet-Navarro J, Rozières A. Differential capacity of human skin dendritic cells to polarize CD4⁺ T cells into IL-17, IL-21 and IL-22 producing cells. *PLoS One*. 2012;7(11):e45680.
13. Fujita H, Nogales KE, Kikuchi T, Gonzalez J, Carucci JA, Krueger JG. Human Langerhans cells induce distinct IL-22-producing CD4⁺ T cells lacking IL-17 production. *Proc Natl Acad Sci U S A*. 2009;106(51):21795–21800.
14. de Jong A, Peña-Cruz V, Cheng TY, Clark RA, Van Rhijn I, Moody DB. CD1a-autoreactive T cells are a normal component of the human $\alpha\beta$ T cell repertoire. *Nat Immunol*. 2010;11(12):1102–1109.
15. Mathers AR, et al. Differential capability of human cutaneous dendritic cell subsets to initiate Th17 responses. *J Immunol*. 2009;182(2):921–933.
16. Lowes MA, Bowcock AM, Krueger JG. Pathogenesis and therapy of psoriasis. *Nature*. 2007;445(7130):866–873.
17. Lande R, et al. Plasmacytoid dendritic cells sense self-DNA coupled with antimicrobial peptide. *Nature*. 2007;449(7162):564–569.
18. Zaba LC, et al. Psoriasis is characterized by accumulation of immunostimulatory and Th1/Th17 cell-polarizing myeloid dendritic cells. *J Invest Dermatol*. 2009;129(1):79–88.
19. Lowes MA, et al. Psoriasis vulgaris lesions contain discrete populations of Th1 and Th17 T cells. *J Invest Dermatol*. 2008;128(5):1207–1211.
20. Chamian F, et al. Alefacept reduces infiltrating T cells, activated dendritic cells, and inflammatory genes in psoriasis vulgaris. *Proc Natl Acad Sci U S A*. 2005;102(6):2075–2080.
21. Lowes MA, et al. Increase in TNF- α and inducible nitric oxide synthase-expressing dendritic cells in psoriasis and reduction with efalizumab (anti-CD11a). *Proc Natl Acad Sci U S A*. 2005;102(52):19057–19062.
22. Sabat R, Ouyang W, Wolk K. Therapeutic opportunities of the IL-22-IL-22R1 system. *Nat Rev Drug Discov*. 2014;13(1):21–38.
23. Nestle FO, Zheng XG, Thompson CB, Turka LA, Nickoloff BJ. Characterization of dermal dendritic cells obtained from normal human skin reveals phenotypic and functionally distinctive subsets. *J Immunol*. 1993;151(11):6535–6545.
24. Gimferrer I, et al. The accessory molecules CD5 and CD6 associate on the membrane of lymphoid T cells. *J Biol Chem*. 2003;278(10):8564–8571.

25. Artyomov MN, et al. Modular expression analysis reveals functional conservation between human Langerhans cells and mouse cross-priming dendritic cells. *J Exp Med*. 2015;212(5):743–757.
26. Breton G, Lee J, Liu K, Nussenzweig MC. Defining human dendritic cell progenitors by multiparametric flow cytometry. *Nat Protoc*. 2015;10(9):1407–1422.
27. Breton G, et al. Circulating precursors of human CD1c⁺ and CD141⁺ dendritic cells. *J Exp Med*. 2015;212(3):401–413.
28. Lee J, et al. Restricted dendritic cell and monocyte progenitors in human cord blood and bone marrow. *J Exp Med*. 2015;212(3):385–399.
29. Seré K, et al. Two distinct types of Langerhans cells populate the skin during steady state and inflammation. *Immunity*. 2012;37(5):905–916.
30. Jostins L, et al. Host-microbe interactions have shaped the genetic architecture of inflammatory bowel disease. *Nature*. 2012;491(7422):119–124.
31. International Multiple Sclerosis Genetics Consortium, et al. Genetic risk and a primary role for cell-mediated immune mechanisms in multiple sclerosis. *Nature*. 2011;476(7359):214–219.
32. Okada Y, et al. Genetics of rheumatoid arthritis contributes to biology and drug discovery. *Nature*. 2014;506(7488):376–381.
33. Zhong W, Zhao L, Liu T, Jiang Z. IL-22-producing CD4⁺T cells in the treatment response of rheumatoid arthritis to combination therapy with methotrexate and leflunomide. *Sci Rep*. 2017;7:41143.
34. Rutz S, Eidenschenk C, Ouyang W. IL-22, not simply a Th17 cytokine. *Immunol Rev*. 2013;252(1):116–132.
35. Leung JM, et al. IL-22-producing CD4⁺ cells are depleted in actively inflamed colitis tissue. *Mucosal Immunol*. 2014;7(1):124–133.
36. Brown MH, Lacey E. A ligand for CD5 is CD5. *J Immunol*. 2010;185(10):6068–6074.
37. de Wit J, et al. CD5 costimulation induces stable Th17 development by promoting IL-23R expression and sustained STAT3 activation. *Blood*. 2011;118(23):6107–6114.
38. Gaublotte JT, et al. Single-cell genomics unveils critical regulators of Th17 cell pathogenicity. *Cell*. 2015;163(6):1400–1412.
39. Wang C, et al. CD5L/AIM regulates lipid biosynthesis and restrains Th17 cell pathogenicity. *Cell*. 2015;163(6):1413–1427.
40. Vera J, et al. The CD5 ectodomain interacts with conserved fungal cell wall components and protects from zymosan-induced septic shock-like syndrome. *Proc Natl Acad Sci U S A*. 2009;106(5):1506–1511.
41. Zhang JG, et al. The dendritic cell receptor Clec9A binds damaged cells via exposed actin filaments. *Immunity*. 2012;36(4):646–657.
42. Sancho D, et al. Identification of a dendritic cell receptor that couples sensing of necrosis to immunity. *Nature*. 2009;458(7240):899–903.
43. Cheung KL, et al. Psoriatic T cells recognize neolipid antigens generated by mast cell phospholipase delivered by exosomes and presented by CD1a. *J Exp Med*. 2016;213(11):2399–2412.
44. Klechevsky E, et al. Cross-priming CD8⁺ T cells by targeting antigens to human dendritic cells through DCIR. *Blood*. 2010;116(10):1685–1697.
45. Maraskovsky E, et al. In vivo generation of human dendritic cell subsets by Flt3 ligand. *Blood*. 2000;96(3):878–884.
46. Yin X, et al. Human blood CD1c⁺ dendritic cells encompass CD5^{high} and CD5^{low} subsets that differ significantly in phenotype, gene expression, and functions. *J Immunol*. 2017;198(4):1553–1564.
47. See P, et al. Mapping the human DC lineage through the integration of high-dimensional techniques. *Science*. 2017;356(6342):eaag3009.
48. Zhang H, et al. A distinct subset of plasmacytoid dendritic cells induces activation and differentiation of B and T lymphocytes. *Proc Natl Acad Sci U S A*. 2017;114(8):1988–1993.
49. Villani AC, et al. Single-cell RNA-seq reveals new types of human blood dendritic cells, monocytes, and progenitors. *Science*. 2017;356(6335):eaah4573.
50. Lewis KL, et al. Notch2 receptor signaling controls functional differentiation of dendritic cells in the spleen and intestine. *Immunity*. 2011;35(5):780–791.
51. Hope JL, Pulendran B, Schoenberger SP, Katsikis PD. 1st International Conference on Human & Translational Immunology. *Nat Immunol*. 2016;18(1):1–4.